REPORT DOCUMENTATION PAGE

AFRL-SR-AR-TR-05-

0505

1. REPORT DATE *(DD-MM-YYYY)*	2. REPORT TYPE	3. DATES COVERED *(From - To)*
December 15, 2005	Final	1 Jul 2003 to 30 Dec 2005

4. TITLE AND SUBTITLE
Molecular Modeling and Experimental Study of Electrocatalytic and Transport Processes in High Temperature Polymer Electrolyte Fuel Cells

5a. CONTRACT NUMBER

5b. GRANT NUMBER
F49620-03-1-0371

5c. PROGRAM ELEMENT NUMBER

6. AUTHOR(S)
Zhou, Xiangyang
Srivastava, Rajiv
Philippidis, G.P.

5d. PROJECT NUMBER

5e. TASK NUMBER

5f. WORK UNIT NUMBER

7. PERFORMING ORGANIZATION NAME(S) AND ADDRESS(ES)
Florida International University
10555 West Flagler Street
TEC 2100
Miami, FL 33174

8. PERFORMING ORGANIZATION REPORT NUMBER

9. SPONSORING / MONITORING AGENCY NAME(S) AND ADDRESS(ES)
AFOSR/NL
875 North Randolph Street
Arlington, VA 22203

10. SPONSOR/MONITOR'S ACRONYM(S)

11. SPONSOR/MONITOR'S REPORT NUMBER(S)

12. DISTRIBUTION / AVAILABILITY STATEMENT
Approve for Public Release: Distribution Unlimited

13. SUPPLEMENTARY NOTES

14. ABSTRACT

15. SUBJECT TERMS

16. SECURITY CLASSIFICATION OF:			17. LIMITATION OF ABSTRACT	18. NUMBER OF PAGES	19a. NAME OF RESPONSIBLE PERSON
a. REPORT	b. ABSTRACT	c. THIS PAGE			19b. TELEPHONE NUMBER *(include area code)*

Final Report

Molecular Modeling and Experimental Study of Electrocatalytic and Transport Processes in High Temperature Polymer Electrolyte Fuel Cells

July 1, 2003 to December 30, 2005

Prepared Under
Grant Award No. F49620-03-1-0371

Submitted to
Air Force Office of Scientific Research
4015 Wilson Building
Arlington, VA 22203

Submitted by
Xiangyang Zhou, Ph.D.
Rajiv Srivastava, Ph.D.
G.P. Philippidis, Ph.D.

Florida International University
10555 West Flagler Street, TEC 2100
Miami, FL 33174

December 15, 2005

TABLE OF CONTENTS

FIGURES CAPTIONS

1.0 Abstract

The molecular dynamic simulation correctly predicted the permeabilities of hydroniums and methanol in a temperature range between 20 and 120°C. The calculated conductivity data gradually deviated from the experimental values with increasing temperature. The deviations were much less than one order of magnitude in wide ranges of temperature and humidity. The permeability of methanol in new ABPBI membranes is much lower than that in the Nafion 117 membrane. The ABPBI membrane is thus promising for use as the polymer electrolyte in a high temperature proton exchange membrane fuel cell. The methods that we used for the *ab initio* atomistic simulations allowed evaluation of the energy barriers for the electrochemical reactions. The *ab initio* simulation results correlated with the experimental results. We also found that $La_{1-x}Fe_{1-y}O_{3-\delta}$ showed significant catalytic activity for methanol oxidation in DMFC. The current sensing atomic force microscopy study allows evaluation of the intrinsic electrochemical activity of electrocatalysts. The results clearly demonstrate that on the catalyst surface areas that are about 20 nanometers to the ionomers are active and the surfaces 50-100 nanometers from the ionomer are not active at all. Only the active sites close to ionomers contribute to the electrocatalysis in a fuel cell.

2.0 Objectives

The ultimate goals of proposed research are to develop computational and experimental techniques for understanding the basic processes of high temperature proton exchange membrane fuel cell (PEMFC) and to identify effective electrocatalysts for JP-8 fuel-fed PEMFC. More specifically, the specific objectives are as follows:

- Develop a computational approach to studying proton conduction, surface diffusion and conduction, catalysis, charge transfer, polarization, and CO-poisoning in the catalyst-electrolyte system;
- Develop experimental approaches to evaluating the transport processes, catalysis, surface diffusion and conduction, charge transfer, polarization, thermodynamics and reaction kinetics at three-phase interfaces, and CO-poisoning in a wide range of temperatures; and
- Reconcile modeling and experimental data to further our understanding of electrocatalysis, poisoning, and transport processes and to help expedite catalyst and PEM selection and optimal design and manufacture of high temperature JP-8 fuel-fed PEMFCs. .

3.0 Status of effort

The project has been completed.

4.0 Summary of Accomplishments/New Findings

According to the project plan, we have accomplished:

1) molecular dynamic simulation of the transport processes in Nafion 117 membranes;
2) development of experimental systems for conductivity and permeability measurement in a wide range of temperature and relative humidity;
3) synthesis of a new type of proton exchange membrane, ABPBI,
4) *ab initio* atomistic simulation of the electrocatalysis processes;
5) development of a high throughput method for evaluating the activity of electrocatalysts;
6) Examination of the Pt electrocatalysts using scanning tunneling microscopy;

7) Exploration of use current sensing atomic force microscopy for evaluating the intrinsic electrochemical activity of electrocatalysts.

The molecular dynamic simulations very precisely predict the permeabilities of hydroniums and methanol in a temperature range between 20 and 120°C. The computational conductivity results gradually deviate from the experimental values with increasing temperature. Overall, the deviations were much less than one order of magnitude in wide ranges of temperature and humidity. The new APPBI membranes are stable at temperature to 110°C. The permeability of methanol in the ABPBI membranes is much lower than that in the Nafion 117 membrane. The PBI membrane is thus promising for use as the polymer electrolyte in a high temperature proton exchange membrane fuel cell.

The methods that we used for the *ab initio* atomistic simulations allow direct evaluation of the energy barriers and reaction rates for electrochemical reactions. The computational results correlate with the experimental results. We also found that a non-precious metal oxide, $La_{1-x}Fe_{1-y}O_{3-\delta}$ showed significant catalytic activity for methanol oxidation in DMFC and were promising for fuel cell applications.

The CSAFM study is the first attempt to evaluate the intrinsic electrochemical activity of electrocatalysts. The results clearly demonstrate that on the catalyst surface areas that are about 20 nanometers to the ionomer are active and the surfaces 50-100 nanometer from the ionomer are not active at all. Only the active sites in these areas actually contribute to the electrocatalysis in a fuel cell electrocatalyst layers.

4.1 Background

Classic atomistic simulation

Nafion (DuPont), a perfluorosulfonic acid polymer, is the most widely studied polymeric electrolyte for proton exchange membrane fuel cell (PEMFC) applications due to its good mechanical properties, chemical stability, and high ionic conductivity. Nafion membranes are used as molecule separators and proton conductors in the membrane electrode assemblies while Nafion ionomers are used in the catalyst layers to promote their electrocatalytic activities. Nafion clusters or thin films in the catalyst layers form the "triple-phase boundaries" (TPBs) that play important roles in the operation of PEMFCs. Modeling and simulation are powerful tools for advancing understanding of PEMFCs and hence development of PEMFC technology. While macroscopic models emphasize transport properties of PEMs and their impacts on fuel cell operations, microscopic models including molecular dynamic (MD) models provide deeper insight of the transport processes such as diffusion and conduction [1]. Although there are many excellent macroscopic models such as irreversible thermodynamic models that bridge the microscopic variables and fuel cell performance, they rely on empirical assumptions and curve fittings. As a result, they are not capable of elucidating the physio-chemical mechanisms as to how molecular structures affect the transport properties and correctly determining the trends of a system which is under conditions outside the ranges (e.g. temperature, pressure, size, water content, etc.) where the curve fittings were done. On the other hand, MD methods use classic or quantum mechanics to predict the behaviors of a system. The predictions are 'exact' in the sense that they can be as accurate as we like, only subject to computational time or computational resource limitations. The present study, we employed MD simulation methods to evaluate the

transport properties of Nafion® polymer electrolytes. Due to computational resource limitations at the time when this study was done, we focused on the simulations of low water content and compared the simulation results with the experimental results.

Ab initio simulation of electrocatalysis

Although the interaction between the fuel molecules and electrocatalysts has been recognized to have a significant effect and an effective control on the electrochemical reactions in PEFCs, a few little researches have been focused on this topic. The primary reason for this may be due to the difficulty in defining the electric double layer (EDL) structure at a solid-polymer interface in comparison with that at a solid-liquid interface. Many state-of–the-art techniques for defining the EDL at solid-liquid interfaces, such as pH titration, electrophoresis, electrokinetics, and electrokinetic sonic amplitude (ESA) methods, are unsuitable for the study of solid-polymer interfaces. Exemplary studies include modeling the charge transfer at a platinum/liquid interface using MP2 and B3LYP programs by Anderson [2], semiempirical modeling of the TiO_2/aqueous solution interface by Machesky [3], and modeling the EDLs and charge transfer at a TiO_2 (rutile)/water interface using a density function theory (DFT) method by Onda et al. [4] It will be a pioneering and challenging task to model and define the interaction between the fuel molecules and electrocatalysts at solid-polymer electrolyte interfaces containing both mobile species and immobile polymer backbones and attached functional groups. It is thus of great academic and practical interest to develop experimental and molecular simulation techniques for elucidate the interaction mechanisms. Better understanding of the interaction between electrode and polymer electrolyte at the molecular level will have a profound impact on many key areas including PEFCs. Furthermore, availability of the validated experimental methods and high throughput computational tools will facilitate the research on the electrocatalysis, enable the rational and innovational design of compatible, durable, and highly effective catalyst and polymer electrolyte couples, and allow timely realization of more efficient and cost effective fuel cells.

Scanning probe microscopy(SPM) study

A SPM is a combination of scanning tunneling microscope and atomic force microscope. SPMs are powerful tools for studying the interaction between the reactants and electrocatalysts in the atomic level [5]. In particular two methods can be used to study the interaction, first, the scanning tunneling microscope with a potentiostat, also known as electrochemical scanning tunneling microscope (EC-STM), and second, current sensing atomic force microscope (CSAFM). The EC-STM allows evaluate the topological changes of the electrocatalysts surface when the electrochemical processes, determine the reaction paths, and quantify the reaction rates. The CSAFM allows detection of the surface current distribution and when works with a potentiostat can evaluate the electrochemistry of a group of molecules on the electrocatalysts.

4.2 Approach

Classic atomistic model

The unit molecular structure for a Dupont Nafion electrolyte is shown in Figure 1. We set m as 8 and the total molecular weight as 1100, which is the same as the value determined in previous studies. At low water contents, the transport processes in Nafion are controlled by single phase diffusion along collapsed paths that connect hydrophilic areas. This allows us to use relatively a smaller number of molecules to construct a molecular model with a sufficient representativeness.

The molecular model was constructed using Materials Studio™ with quantum chemistry and MD modules. The first step is to construct individual molecules including H_2O, H_3O^+, H^+, methanol, and Nafion repeating units that have two branches. The structures of the molecules are illustrated in Figure 2. These molecules were optimized using the quantum chemistry module (VAMP™) to have minimum total energies. Then, the optimized molecules were included into a unit cell for a periodic boundary condition. The unit cell was then optimized in the pcff force field [1] to allow the total interaction potential to converge to a minimum. The compositions and properties of the unit cells are summarized in Table 1. The water content is defined as the molar ratio of water to the sulfonated group in Nafion. Water content and density are functions of relative humidity. These functions are evaluated using the following empirical laws [6, 7]. Although the activity of liquid water is 1.0 or 100%, the conductivity of the Nafion was reported to be greater than the conductivity of Nafion in water vapor at 100%. This is known as the Schroeder paradox. Weber and Newman [6, 7] explained this paradox using a continuum physical model that describes the change of water containing pore structure as a function of relative humidity and the difference between the pore structures in water vapor and in liquid water. The model was established using a series of assumptions, master equations, and a few unpredictable parameters, such as the tortuosity of the pores, the dynamic viscosity of water in the pores, the dielectic constant of water in the pores, etc. As shown in Figure 3, the unit cell with water content of 3 contains some isolated water domains where the water domains in the unit cell with water content of 22 are interconnected. The hydrophilic sites or sulfonate acid groups do attract several water or hydronium molecules in their vicinities.

Table 1. Parameter set for the molecular dynamic simulations

Unit cell	A	B	C
Water content, λ, room temperature	3	13	22
Density, g cm^3	2.0	1.7	1.5
Relative humidity	50%	100%	Liquid water
No. of Nafion repeating unit	10	10	10
No. of H_2O	20	120	210
No. of H_3O^+	7	7	7
No. of H^+	3	3	3
No. of CH_3OH	4	4	4

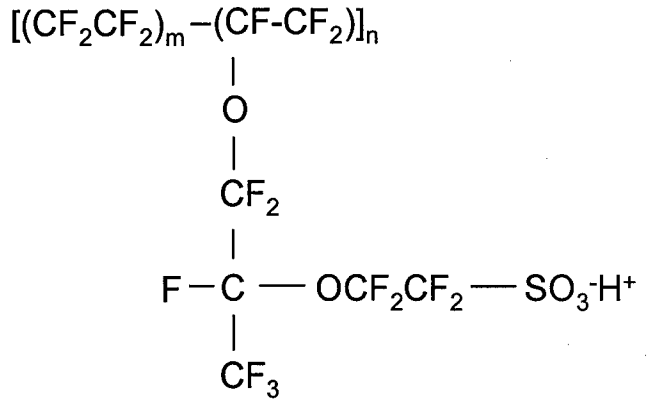

Figure 1 . Unit molecular structure for a Dupont Nafion electrolyte.

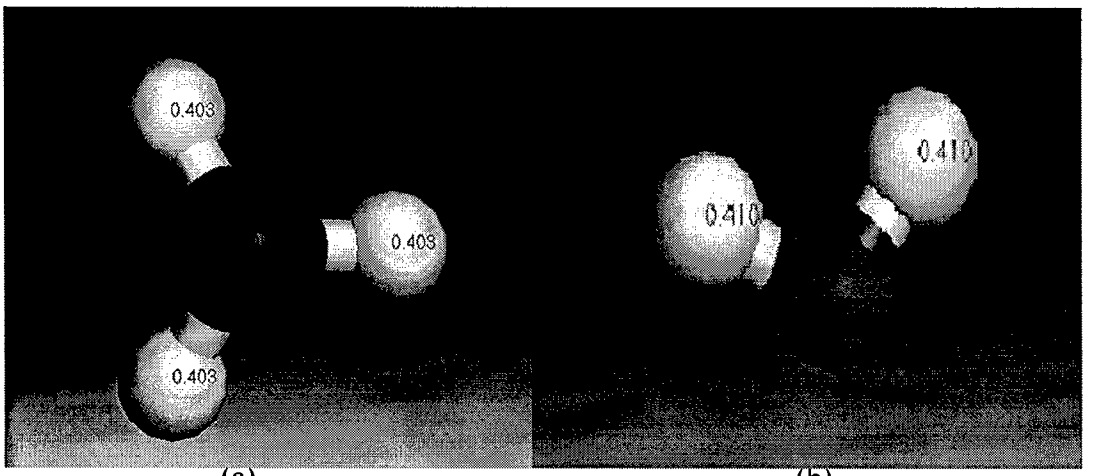

(a) (b)

(a) (b)

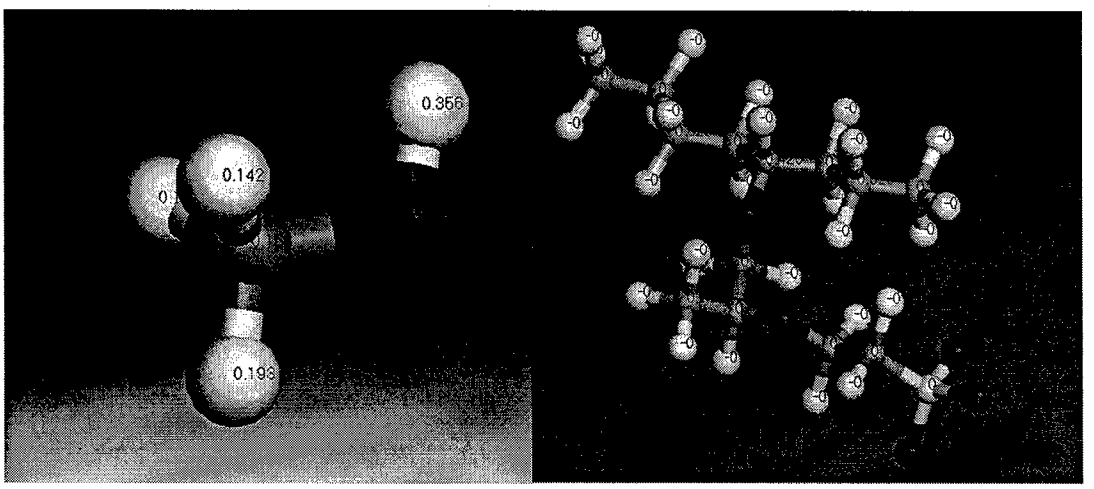

(c) (d)

Figure 2. Structures of hydronium, water, methanol, and Nafion created using MS.

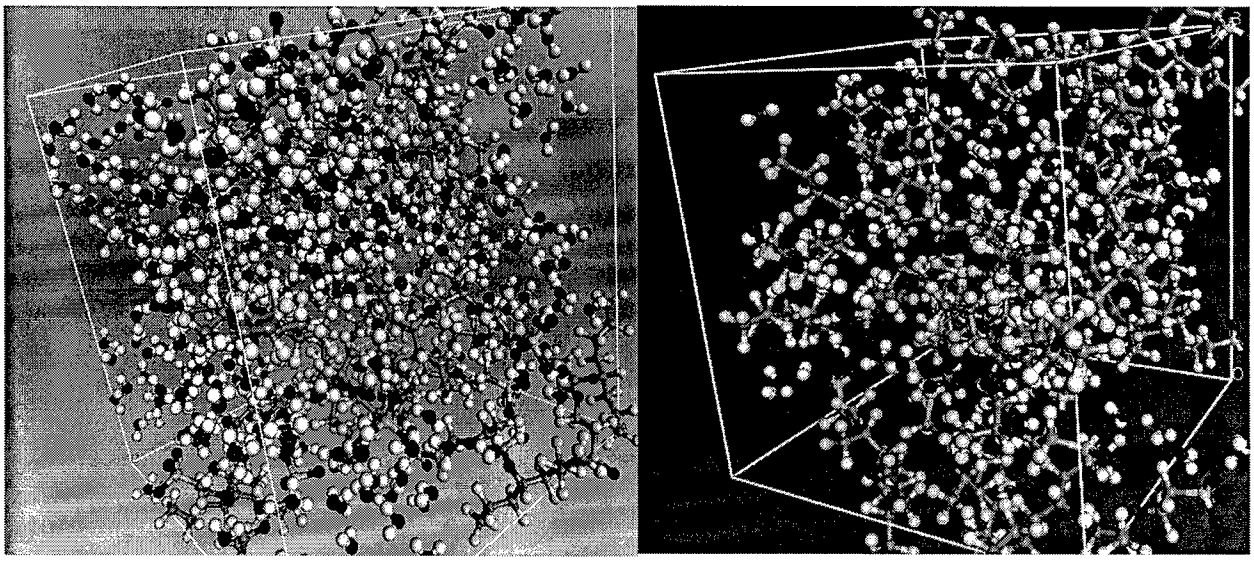

Figure 3. Two model repeating unit cells. Left: λ=22; and right: λ=3

Classic molecular dynamic (MD) simulation

Using the MD simulation module, Discover™, we set the system at a temperature between 298.15 to 423.15°K under NVE ensemble with constant particle number, constant volume (1 bar), and constant temperature. The water uptakes or water contents were fixed at 3, 13, or 22 H_2O/SO_3^-, which correspond to the water uptakes at 50% relative humidity (RH), at 100% RH, and in liquid water respectively. The initial velocity was randomly determined according to Boltzmann statistics. The time step was set at 1.0 fs and duration at 200 ps in which equilibrium states were reached.

Conductivity measurement

Conductivity measurements were conducted using an apparatus (Figure 4) similar to that described in our previous publication. However, the present apparatus is equipped with a dry air generator, a HPLC pump, and a high temperature humidity transducer. By manually adjusting the dry air and pure water flow rates, the relative humidity or water partial pressure can be controlled with a precision of ± 5%. The impedance of the membrane was measured using a four-probe AC method. The resistance between two Pt probes that contact with the membrane

was measured using a Solartron electrochemical measurement system with a precision better than ± 1%. The conductivity is evaluated using [8]:

$$\sigma = \frac{1}{R} \times \frac{h}{S} \qquad \text{Eq. (1)}$$

where R is the resistance of the membrane, h is the membrane thickness, and S is the cross section of membrane.

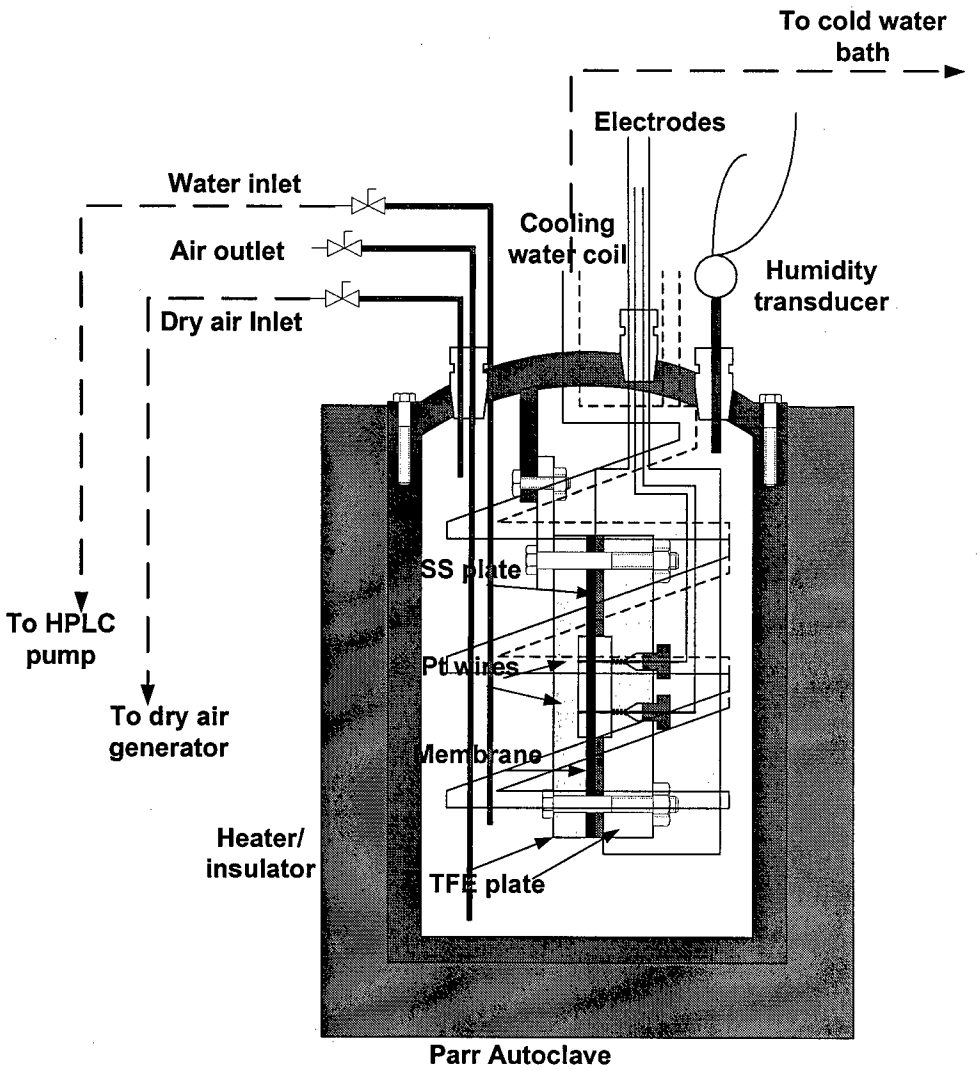

Figure 4. Experimental schematic used for the conductivity experiments.

Permeability measurement

This apparatus consists of a membrane diffusion cell and a pressure balance cell. As shown in Figure 5, the two chambers of the membrane diffusion cell are separated with the membrane to be studied. The two chambers of pressure balance cell are separated with a thick (1.5 mm) flexible rubber sheet. One of the chambers is filled with a solution (e.g. 3 M methanol solution or hydrogen in nitrogen) while the other chamber is filled with a pure solvent (e.g. deionized water or nitrogen). Because the pressures in the two chambers are equalized by the pressure balance cell, the solute passes through a polymer membrane via molecular diffusion. The pressure is controlled with a pressure relief valve. The temperature in the membrane diffusion cell is controlled with a thermocouple, heating tape, and temperature controller. The solution concentration is kept constant by constantly pumping fresh solution into the solution chamber. Samples are taken by syringe from the solvent chamber once the solution had been pumped through the lower chamber for 3½ hours. A sampling port is installed to the left chamber that initially contained pure water. The methanol, thus, diffuses from the right to the left chamber through the proton exchange membrane at a zero pressure difference between the chambers. The permeability of the membrane is evaluated using [9]:

$$K = HD = \frac{lV_{sample}}{At_{\exp}} \ln \left| \frac{C_1 - C_{methanol}}{C_2 - C_{methanol}} \right| \qquad \text{Eq. (2)}$$

where D is the diffusion coefficient, H is the partition coefficient, the product DH is the methanol permeability, C_1 is the methanol concentration in the left chamber at the beginning of the experiment (t=0), C_2 is the methanol concentration in the left chamber by the end of the experiment ($t=t_{exp}$), $C_{methanol}$ is the methanol concentration in the right chamber, which is a constant, A and l are the exposed area and thickness of the membrane, and V_{sample} is the volume of the left chamber.

Synthesis of poly(2,5-benzimidazole) ABPBI membrane

The apparatus (Figure 6) for polymer synthesis is modified from a Parr Instrument high pressure vessel with automatic controls for heating and cooling. Initial organic solutions were contained in a Teflon beaker and mixed with a magnetic driven impeller. The method for synthesizing AB-PBI is illustrated in Figure 7. ABPBI was obtained by condensation of 3,4-diaminobenzoic acid monomers in polyphosphoric acid (PPA). The polymerization was carried out heating a solution of 3.040 g (20 mmol) of 3,4-diaminobenzoic acid in 50 g of PPA (85% P_2O_5) at 200 °C for 5 h under nitrogen. The polymer was isolated by precipitation in water, filtered, and washed repeatedly with water. To eliminate residual phosphoric acid, the polymer was washed with 10% NaOH stirring overnight. The dark purple polymer became brown after the NaOH addition. NaOH was eliminated by washing with water to neutrality and boiling the polymer in water for 6 h, three times. The purified polymer was dried at 100 °C for 24 h and 200 °C for another 24 h. A brown fibrous polymer was obtained. The polymer was then dissolved in methanesulfonic acid and doped with concentrated phosphoric acid. Membranes can be cast when the solvent is partially vaporized. Initial experimental results indicate that these membranes are flexible and sufficiently strong. The conductivity can be 0.05 S cm^{-1} under ambient conditions. This is similar to the conductivity of a typical Nafion 117 membrane under the same condition.

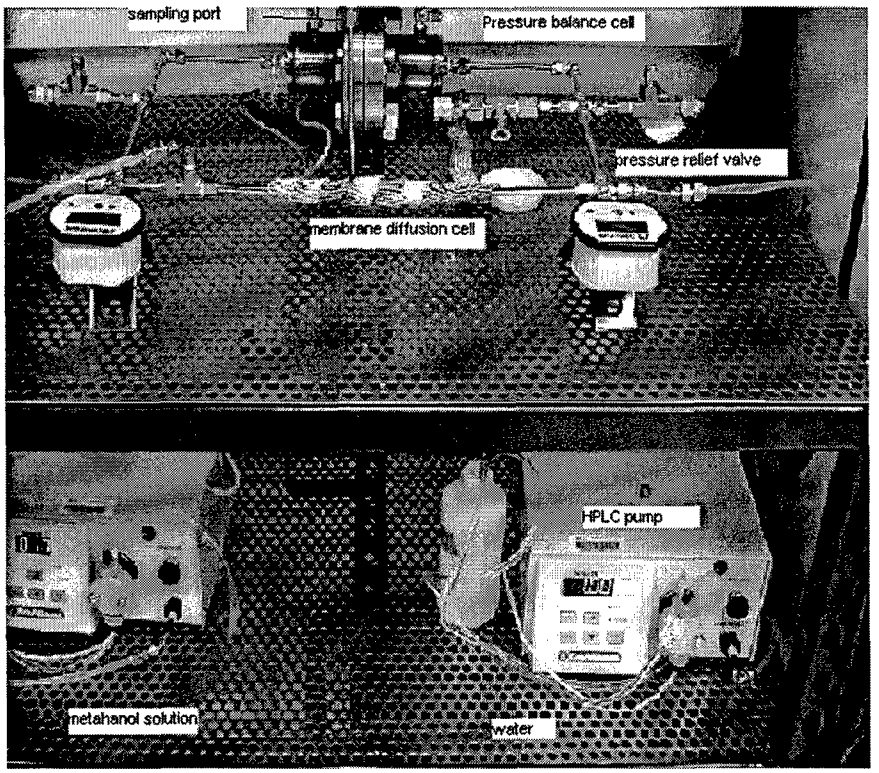

Figure 5. Apparatus for permeability measurements at elevated temperatures

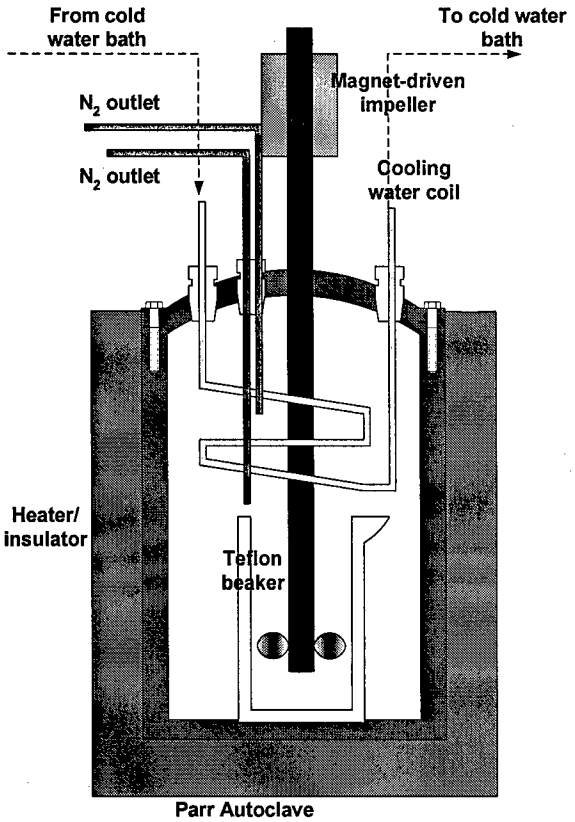

Figure 6. Schematic of the apparatus for membrane synthesis at elevated temperatures.

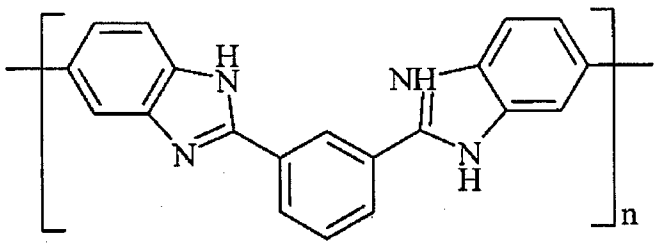

Polybenzimidazole (PBI)

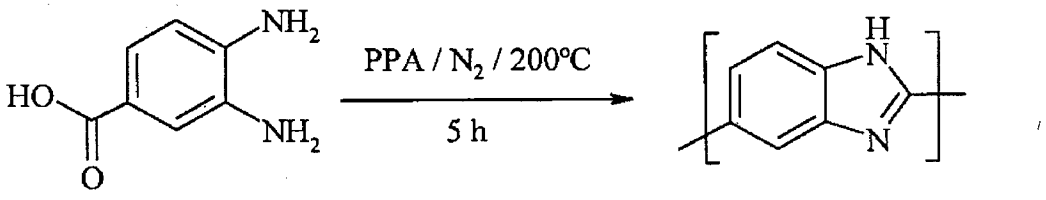

3,4-diaminobenzoic acid (DABA)

Poly(2,5-benzimidazole) (ABPBI)

Figure 7. Reactions for ABPBI, MPPBBI and SMPPBBI synthesis.

Ab initio Simulation of Electrochemical Reactions on Electrocatalysts

In the present work we focused on the adsorption and bond breaking processes of methanol on electrocatalysts, Pt, $LaFeO_3$, and $LaMnO_3$. First of all, a crystal surface model of the catalyst material was created using Materials Studio (Figure 8). A methanol molecule was added above the surface. Then, a final configuration (product) of the adsorption and bond breaking reaction was created (Figure 9). Both configurations were optimized using CASTEP [10]. Finally, the reaction paths and reaction energies related to the paths are evaluated. The path with the minimum energy barrier is identified using the linear synchronous transit (LST) and quadratic synchronous transit (QST) algorithm [10]. The computation results are compared with the electrochemical measurement results.

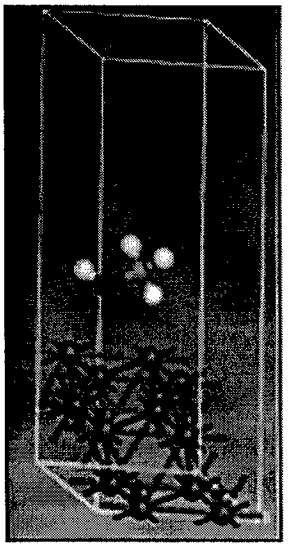

Figure 8. Model of Pt surface and a free methanol molecule(initial configuration).

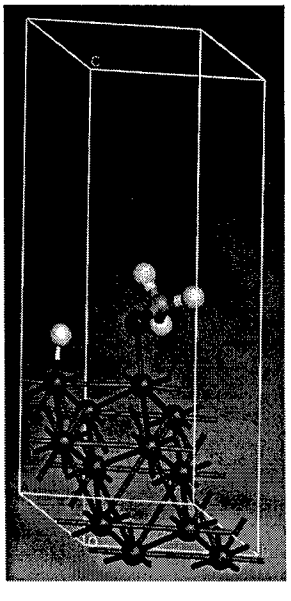

Figure 9. A hydrogen atom is separated from the adsorbed methanol molecule on the Pt surface (final configuration).

Electrochemical measurements for evaluating electrocatalysts

As shown in Figure 10, an electrochemical cell was designed for high throughput evaluation of the electrocatalysts. The bottom parts of the Nafion membrane electrode assembly or the anode was immersed into 1 M methanol solution while the cathode and reference electrode were exposed in air (Figure 10). Thus, the setup mimics the testing conditions in a direct methanol fuel cell (DMFC). Cyclic voltametry measurements were conducted using a Solartron 1287 Electrochemical Interface and 1260 Impedance/Gain-Phase Analyzer.

The membrane electrode assembly (MEA) was fabricated with a Nafion 117 membrane (4 x 4 cm^2) as the electrolyte sandwiched by two L-shaped carbon cloth (E-Tek)-based electrodes (Figure 10). The anode (working electrode) loaded with perovskite, Pt, or Pt/Ru ink, was 3 x 4 cm^2 with a 0.5 x 2.5 cm^2 corner being cutoff. The cathode (counter electrode) loaded with Pt ink was 1 x 4 cm^2 with a 0.5 x 2.5 cm^2 corner being cutoff. The loadings of the perovskite, Pt-Ru or Pt were 2.0 ± 0.5 mg cm^{-2}. A silver wire coated with silver chloride was used as the reference electrode. The relative orientation of the working and counter electrodes was such that they were placed on the opposite upper corners of the two sides of the membrane. The assembly was then hot pressed at 100°C and 2000 psi for 6 minutes. The reference electrode was tied to the membrane and then hot pressed into the membrane in the same way. The resistances between the electrodes were evaluated using impedance spectroscopy. Typically, resistance between the working and counter electrodes was 0.2 Ω, while that between the reference and working electrodes was 1.5 Ω.

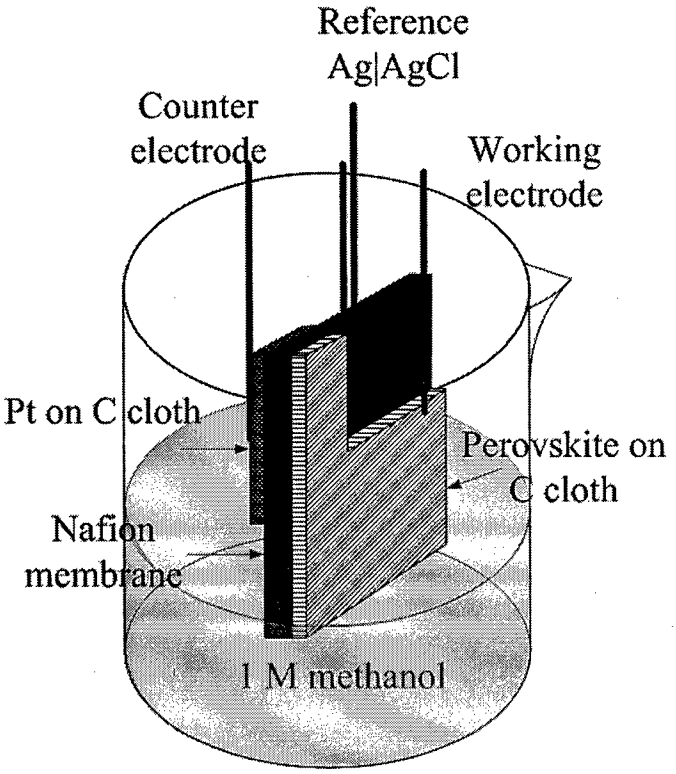

Figure 10. Schematic of the experimental setup for evaluating the electrocatalytic activity of the perovskite materials.

STM study of the Electrocatalysts

Metal particles on the nanometer scale are used as catalysts or electrocatalysts in many heterogeneous catalysis processes, and have attracted considerable attention recently [11-13]. The dependence of activity and selectivity for catalytic reactions of Pt on the structure, size, and morphology of crystallites has been widely investigated [14-16]. Previous results indicate that Pt has maximum activity when 3~5nm in size [15], and that the size of Pt particles is only important when the intercrystallite distance is less than 20 nm [16]. In recent years, scanning tunneling microscopy (STM) has become a promising technique to obtain structural information about electrochemical interfaces at the atomic level. Many significant results for the electrodeposition of metals [17-19] have been found due to the STM's ability to view nanostructures one to several atomic layers thin, and extensive progress [20, 21] in the understanding of the microscopic nucleation and growth of metal particles has been made. A large variety of the microtopographies with specific electrocatalytic properties has been observed on the Pt electrodeposited from H_2PtCl_6 on carbon substrates [14, 18, 22] at a certain overpotential. This work presents the formation of Pt with a very narrow distribution of nanocrystallite particle size through the process of electrochemical deposition from H_2PtCl_6 solutions without a supporting solute.

Pt electrochemical deposition was carried out on highly oriented pyrolytic graphite (HOPG) substrates. An aqueous 0.01M hexachloroplatinate acid (Alfa Aesar, 99.9%) solution was used. All solutions were prepared from reagent grade (A.R.) chemicals and deionized water (18MΩ cm resistivity). Deposition condition control of the working electrode was achieved with a pico-potentiostat (Molecular Imaging). After completion of electrochemical deposition, samples were gently rinsed with deionized water and methanol before being dried with flowing air at room temperature. Pico STM was used to image the samples at room conditions.

A conventional three-electrode cell with a Ag/AgCl reference electrode was used. Any dust particles were removed from the surface of the HOPG with a quick application and removal of adhesive tape prior to each experiment. A Pt wire (0.5 mm diameter) was used as a counter electrode. One drop of H_2PtCl_6 solution (10mM) without a supporting solute was dripped onto the HOPG. The potential of the HOPG surface was swept from –0.5 V to 0.8 V with a rate of 20 mV/s. A typical cyclic voltammogram (CV) of the HOPG surface is presented in Figure 11. The deposition was performed with a bias voltage of –200 mV at 60 s. STM observation found that nucleation of Pt particles begins at surface defects such as surface steps. The low-resolution STM images of Pt deposits grown within the potential window used in this work are characterized by a number of separate Pt agglomerates and large, bare HOPG surface domains.

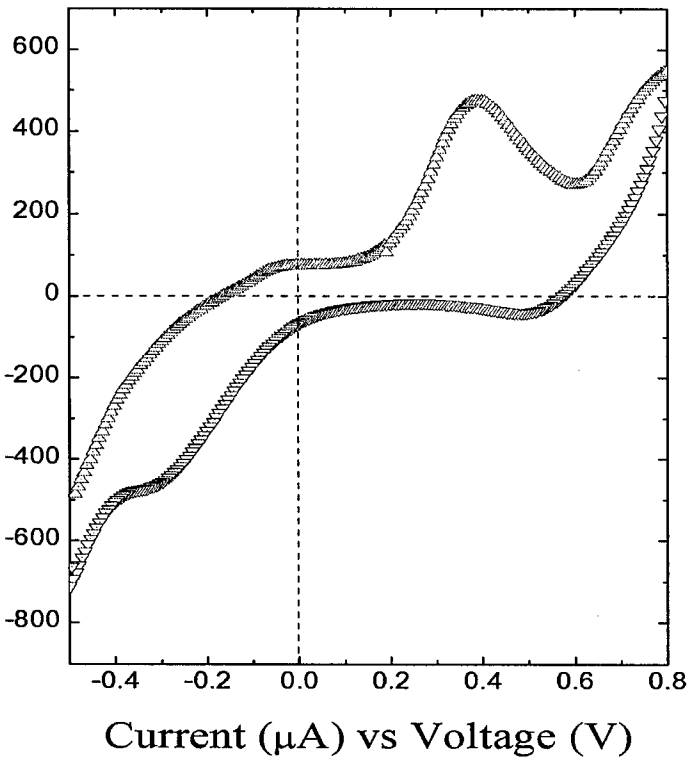

Figure 11. Cyclic voltammogram of a HOPG surface in H_2PtCl_6 solution (10mM).

CSAFM study of electrocatalysts on Nafion membrane

So far, there is no reliable method that proves reliable for evaluating the electrochemical activity of single catalyst particle. Both fundamental and applied researches rely on empirical approaches to evaluate the intrinsic activity of the electrocatalysts. As shown in Figure 12. a conductive AFM tip was used as a current collector on the electrocatalysts. The electrocatalysts were loaded on a Nafion membrane that itself was attached on a Pt sheet as the counter electrode. The detected current from the electrocatalysts is the indication of the activity of the electrocatalysts.

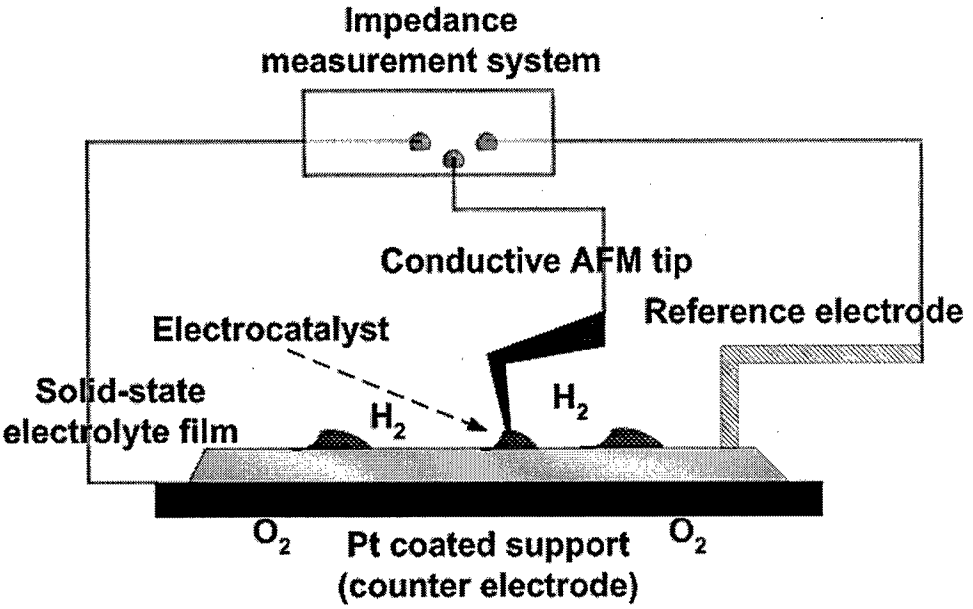

Figure 12. Experimental setup for CSAFM and AFM impedance measurements.

4.3 Results

Molecular dynamic simulation results

Each run of the molecular dynamic (MD) computation lasts roughly 72 hours using a Dell Pentium IV personal computer. The position vector of each particle, is saved as a function of time. The Einstein equation was used to calculate the ionic conductivity, σ [10],

$$\sigma = \frac{e^2}{6tVkT}\left(\sum_i z_i^2\left\langle[R_i(t)-R_i(0)]^2\right\rangle + 2\sum_{j>i} z_i z_j\left\langle[R_i(t)-R_i(0)][R_j(t)-R_j(0)]\right\rangle\right) \qquad \text{Eq. (3)}$$

where t is the time, V, the volume of the unit cell, e, the electronic charge, k, Boltzmann's constant, T, the temperature, and z, the charge of the ions. An exemplary original simulation run are shown in Figure 13. The simulation results are consistent to the nuclear magnetic resonance measurement (NMR) results (Table 2). We also found that the diffusivity of hydronium is similar to that of proton. This phenomenon is investigated by tracking the trajectories of the protons in the unit cells. As shown in Figure 14, a proton is entangled with a water molecule in its path moving from one to another sulfonated group. Thus, the proton and the entangled water as a whole behave like a hydronium.

The molecular dynamic simulation models were established using the *ab initio* optimization computation and just two empirical laws that evaluate the density and water content at a specific relative humidity or in liquid water. The molecular dynamic simulations based on force fields can be viewed as "tests" in a virtual space. The motions and interactions between the molecules

can be studied in a microscopic scale. The macroscopic transport processes of all species can be evaluated using the statistical methods. In the present simulations, no additional assumption is made in order to explain the Schroeder paradox. The simulation results indicate that conductivities in liquid water and in water vapor with 100% relative humidity are different although the activity of water in both liquid water or in the vapor with 100% relative humidity is 1.0. Many efforts [6,7] have been made to elucidate the mechanisms of proton conduction. The state of proton in Nafion is still the center of disputes. The present simulation results show that "free" protons and hydroniums have similar diffusivity or conduction because the protons are really not free but are entangled with a water molecule in a substantial period of time. Thus, the proton and the water molecule that is entangled with the proton are equivalent to a hydronium in transporting positive charges.

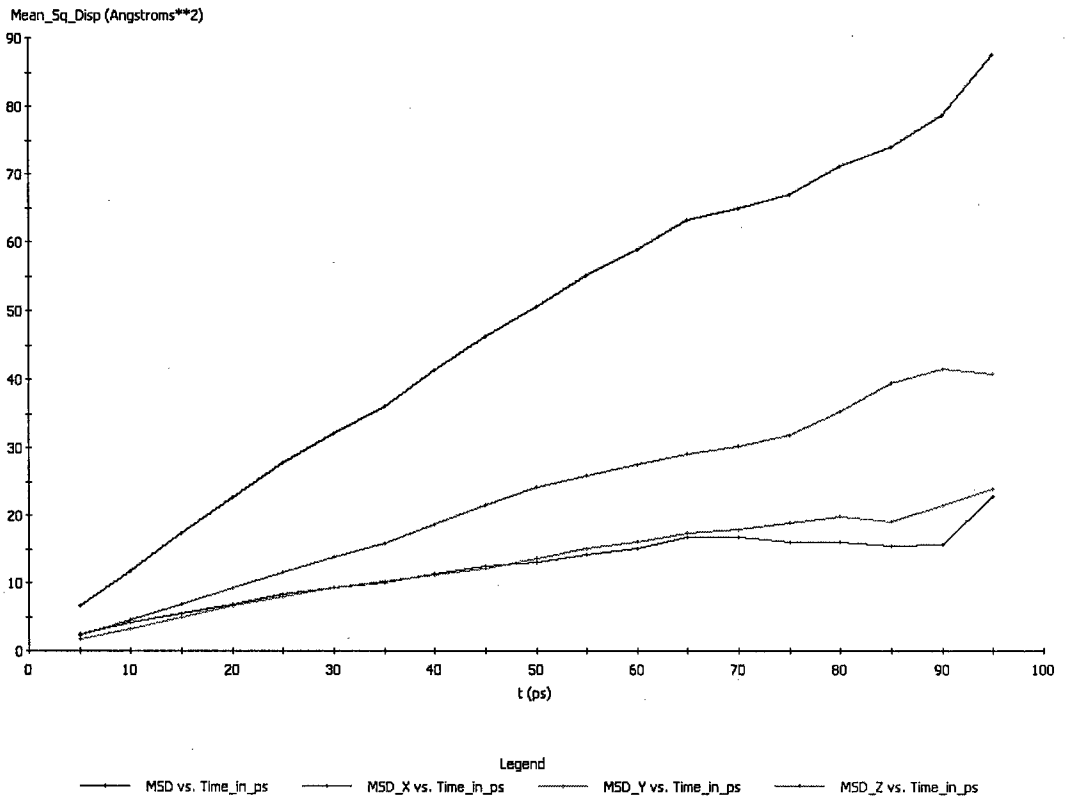

Figure 13. Results from a simulation run. The mean square displacement of protons in the model unit cell is presented as a function of simulation time.

Table 2. Simulation and Nuclear magnetic resonance (NMR) results from literature [23].

Water content	D_{H3O+} (cal.) $cm^2 s^{-1}$	D_{H3O+} (Exp.) $cm^2 s^{-1}$
Low (λ =3)	4.62×10^{-6}	$2.0 \times 10^{-6} \sim 6.0 \times 10^{-6}$
High (λ =13)	1.11×10^{-5}	$7.0 \times 10^{-6} \sim 1.0 \times 10^{-5}$

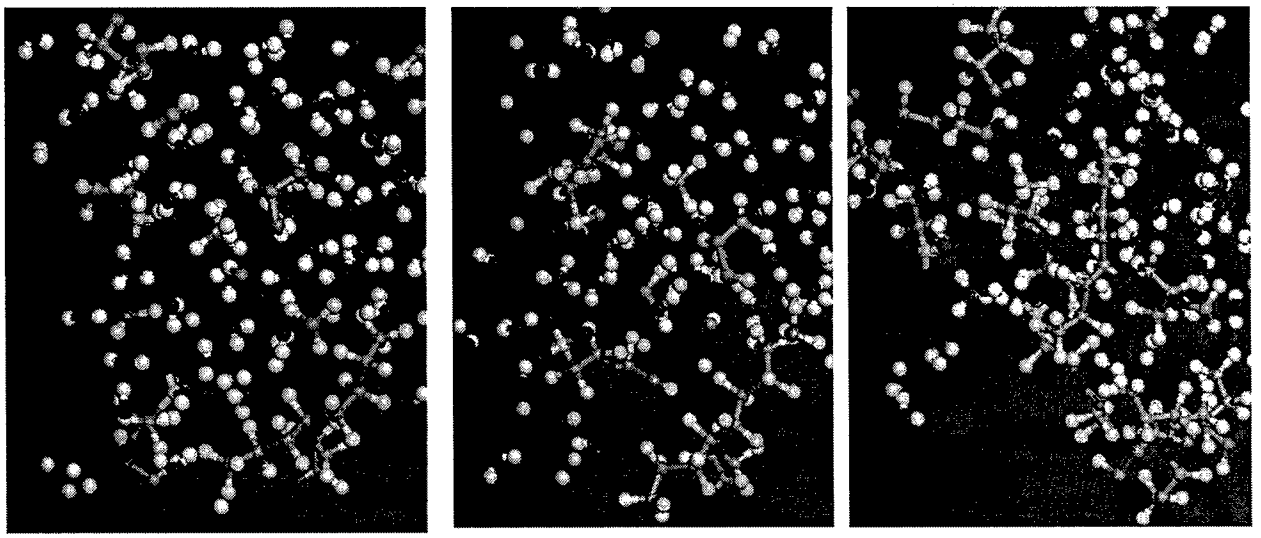

t=0.0 s t=175 ps t=500 ps

Figure 14. A cartoon that shows a proton (blue) is entangled with a water (pink and gray) when it is traveling in Nafion.

Conductivity measurement results

The results of 15 runs using the model unit cells A, B, and C are presented in Figure 15 with the open symbols where the experimental results are presented with the close symbols. The diffusivity of hydroniums evaluated using the simulation models is in good agreement with the diffusivity of hydroniums evaluated using nuclear magnetic resonance (NMR) [23].

Methanol permeability measurement results

Figure 16 shows the simulation and permeability measurement results. The experimental results are very close to the results that were obtained previously [9]. The methanol diffusivity data that evaluated using the atomistic simulation method are generally slightly greater than the experimental permeability results. If the partitioning coefficient, H, in Eq. (2), is close to 1.0, the simulation and experiment results are in very good agreement.

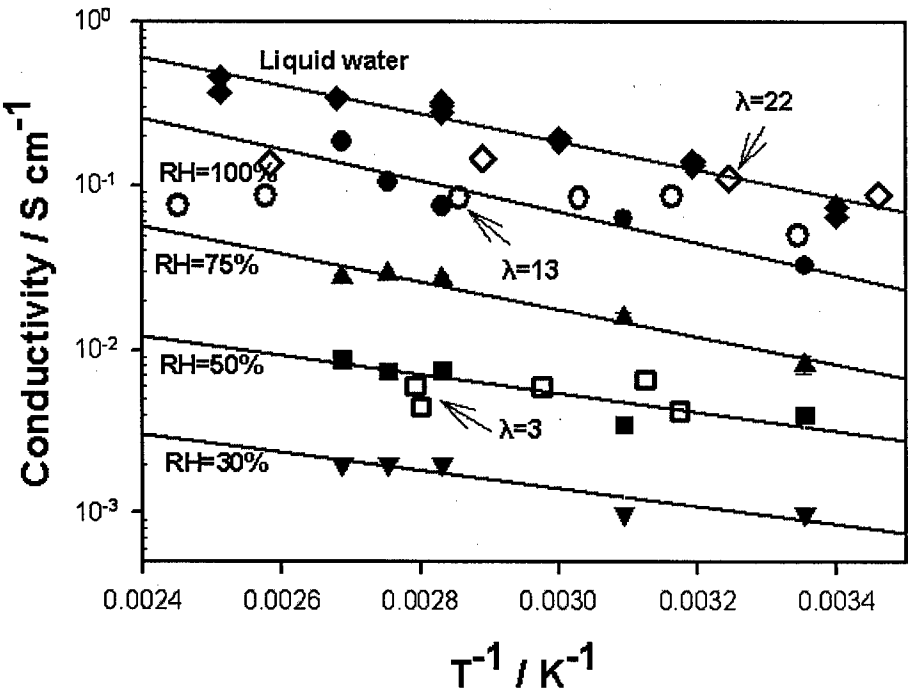

Figure 15. Conductivity as a function of temperature and relative humidity and results of atomistic simulation.

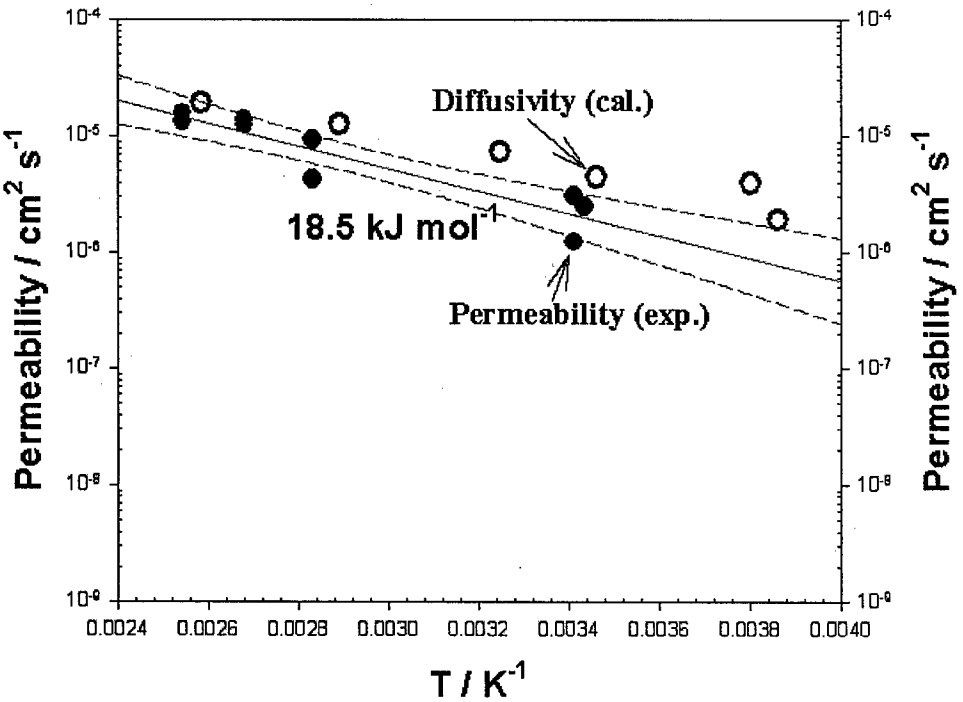

Figure 16. Methanol permeability as a function of temperature and diffusivity data evaluated using the atomistic simulation method.

MD simulation versus experimental study

The simulation results are consistent with the experimental results at lower temperature range from 25 to 77°C. At higher temperatures, there are significant differences between the simulation and experimental results. The primary reason for this discrepancy is that these simulation models do not take into account and interaction between the membrane itself and its environment. In reality, the water uptake at elevated temperatures may be greater than that at room temperature. This was evidenced with the observations that after a membrane experienced elevated temperatures between 60 and 90°C, the membrane expanded considerably. Thus, the water content may increase with temperature, in particularly for liquid water environment. This can explain why the discrepancies between the computational and experimental results in liquid water are greater than those in gaseous environment. The second reason is that the combination of the protons in the sulfonated group with water may be a function of temperature. The combination of proton with water or hydrolyzation of proton is thought to result in "free" positive charge carriers and hence to be b the pre-requisition for proton conduction [24]. The present simulation models do take this into account. The third reason is that the size of the atomistic models is not big enough to account for proton transport that is related to water flow in nana-channels. After all, the experimental and computational results demonstrate that the conductivity of the Nafion membrane can be determined within one order of magnitude in a temperature range between 20 and 80°C using the molecular dynamic simulation method.

The simulation models correctly predict the diffusivities of hydronium and methanol in a wide range of temperature. Unlike conductivity, the permeability or diffusivity of a species is insensitive to the concentration of the species. Thus, increase of number of "free" protons or hydrolyzed protons will not significantly impact the diffusivity of proton or hydronium. Methanol is a neutral species and weakly interacts with Nafion backbone. It is not a surprise that the present MD models that do not consider chemical interaction between the molecules can correctly evaluate the diffusivity of methanol. Because the present experimental setup is limited for liquid samples, whether or not the permeability of diffusivity is strongly depends on water content has not been examined.

The present results demonstrate that molecular dynamic simulation can correctly mimic the transport processes of a proton exchange membrane and can be used for expedition of new proton exchange membrane for future more effective PEMFCs. It is very interesting that this method is used to predict other existing or even virtual polymer electrolytes that are created in computer according to quantum chemistry laws.

Conductivity and permeability of poly(2,5-benzimidazole) ABPBI membrane

As shown in Figures 17 and 18, the conductivity of the ABPBI membranes was generally lower than that of the Nafion membrane. However, the conductivity of the Nafion membrane in 100% humidity vapor was quickly reduced to zero when the temperature was increased above 100°C. In the case of the ABPBI membranes, the conductivity was almost a constant. The permeability of the ABPBI membrane was much lower than that of the Nafion membrane. These properties of the ABPBI versus the Nafion membrane can be utilized to fabricate more effective high temperature proton exchange membrane fuel cells.

Error!

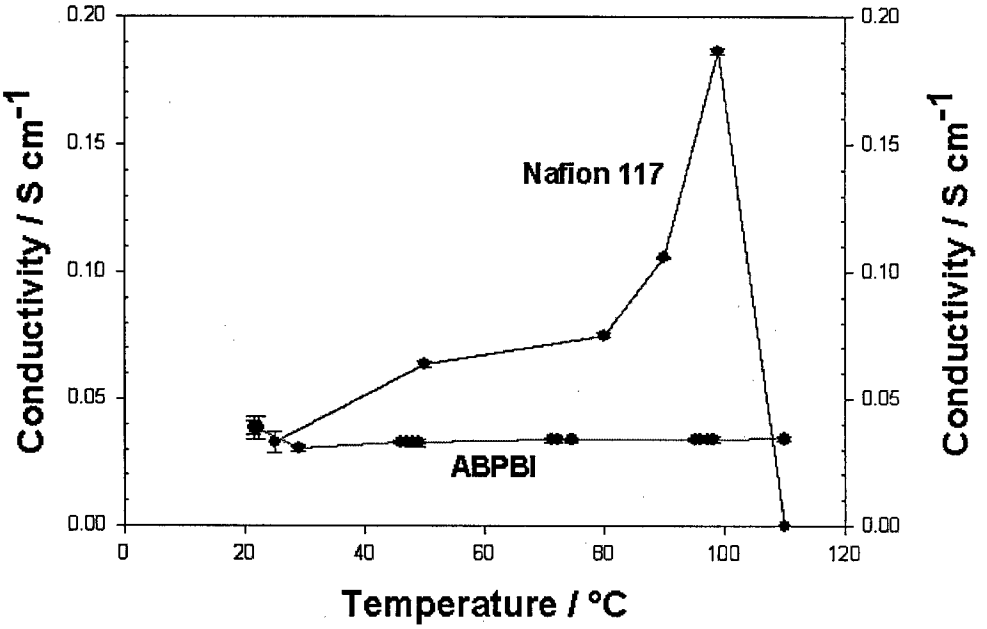

Figure 17. Conductivities of Nafion and ABPBI as functions of temperature at 100% relative humidity.

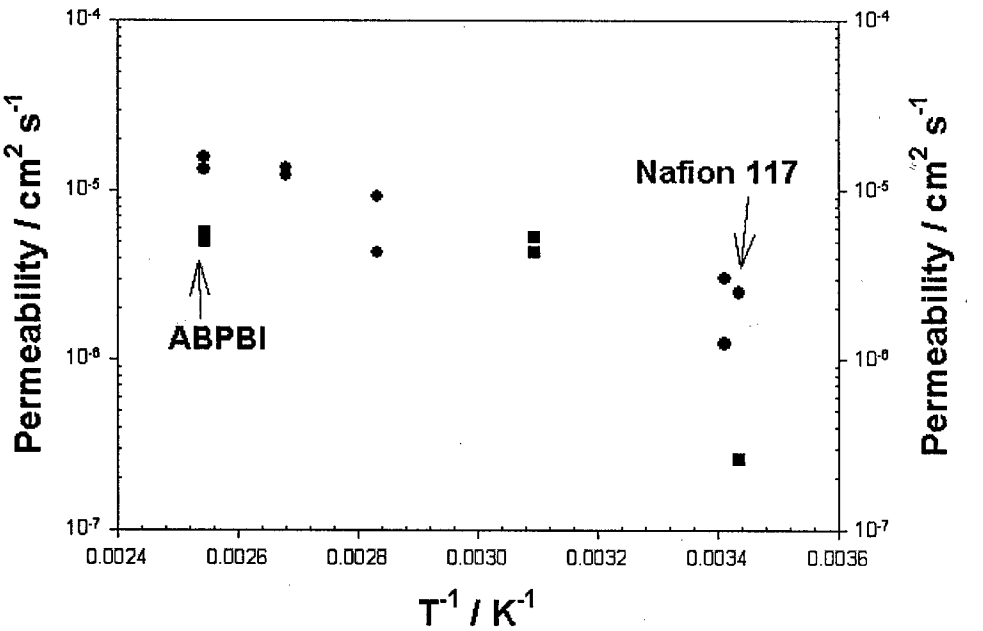

Figure 18. Methanol permeability in Nafion 117 and ABPBI membranes.

Ab initio simulation of electrocatalysis and electrochemical measurements

LST and QST allow search and define the possible reaction paths and the energy barrier for each specific reaction path. The search procedure consists of many small displacements from the previous configuration. Small variations are applied to these displacements for a quest for the minimum energy barriers. Because for each small variation of the configuration the solutions of the Schrödinger equation have to be re-evaluated, the computation time for evaluating the reaction paths and energy barriers was as long as 840 hours. Figure 19 illustrates the initial, final, and transition configurations evaluated using the *ab initio* methods. The transition state at the bottom reflects a reaction path in which first, the methanol is adsorbed on the Pt surface, then, the O-H bond break, and finally, the H atom is adsorbed on the Pt surface. On the other hand, the transition state on the top reflects a different scenario. The hydrogen atom of the O-H bond first interact with the neighboring Pt atom and form a H-Pt bond and then break from the O-H bond. The formation of the H-Pt bond reduces the energy required for breaking the O-H bond. The maximum and minimum energy barriers for Pt, $LaFeO_3$, and $LaMnO_3$ are listed in Table 3.

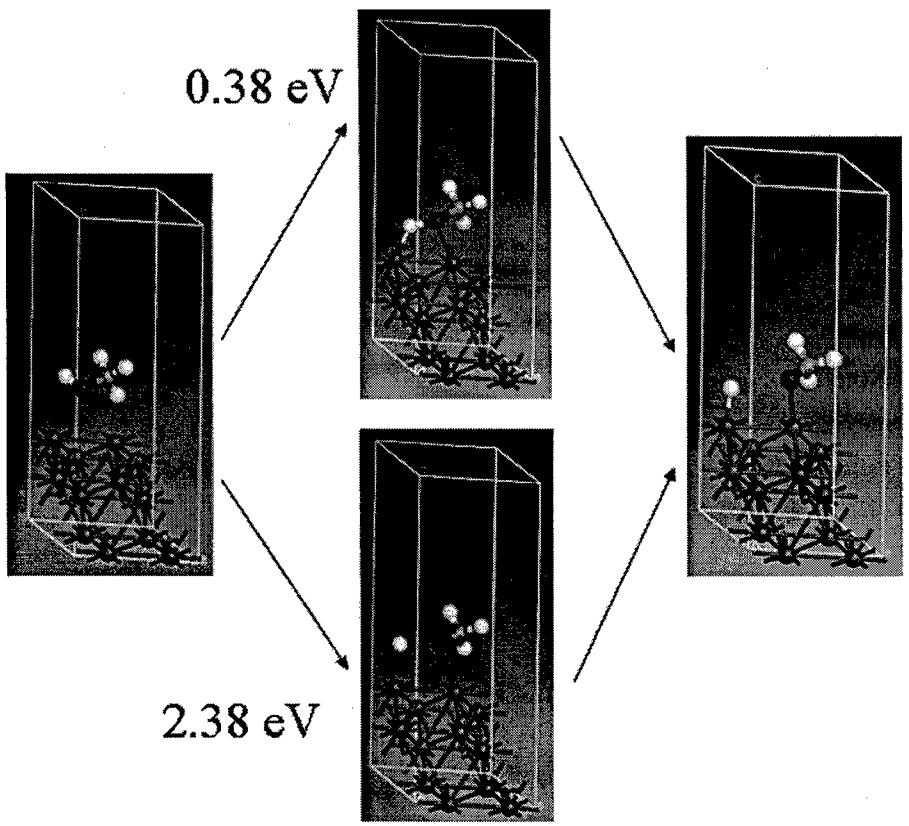

Figure 19. *ab initio* modeling of methanol oxidation processes on Pt, $LaMnO_3$, and $LaFeO_3$.

Table 3. Minimum and maximum energy barriers for different electrocatalysts.

Materials	Minimum Energy Barrier / eV	Maximum Energy Barrier / eV
$LaMnO_3$	1.45	33.8
$LaFeO_3$	0.84	4.08
Pt	0.38	2.38

Cyclic voltametry tests were conducted at a scanning rate of 25 mV s^{-1}. Two identical MEAs were tested for each electrocatalyst material. The current-voltage curves are illustrated in Figure 20. Among the perovskite materials, only $La_{1-x}Mn_{1-y}O_{3-\delta}$ and $La_{1-x}Fe_{1-y}O_{3-\delta}$ showed satisfactory stability in methanol solutions as the current densities for these two materials did not decrease with the number of cycles. The methanol oxidation onset potentials and apparent exchange current density are summarized in Table 4. The current density detected from a piece of blank carbon cloth was very low and was deemed to be catalytically inactive. The methanol oxidation onset potential for $La_{1-x}Fe_{1-y}O_{3-\delta}$ was the most cathodic among all the materials tested, indicating an easier initiation of methanol oxidation on $La_{1-x}Fe_{1-y}O_{3-\delta}$. The exchange current density for $La_{1-x}Fe_{1-y}O_{3-\delta}$ was 20% greater that that of Pt/C but 50% lower than that of Pt-Ru/C. Some electrocatalytic activity for methanol oxidation was observed on $La_{1-x}Mn_{1-y}O_{3-\delta}$ but the activity was much lower than that observed on $La_{1-x}Fe_{1-y}O_{3-\delta}$. While $La_{1-x}Fe_{1-y}O_{3-\delta}$ shows significant catalytic activity for methanol oxidation in DMFC, this was achieved at a relatively low specific surface area and without interface optimization. An electrochemical reaction including methanol oxidation at the anode of a fuel cell can be divided into many reaction steps in parallel or in series. Adsorption, bond breaking, charge transfer, and charge transport are the major steps of the electrochemical reaction. The slowest step determines the reaction rate. Which step is the rate determining step or rds a subject of extensive disputes. In the present research, we found that the methanol oxidation onset potential generally correlated with the energy barrier for the adsorption and bond breaking. The onset potentials of Pt and $La_{1-x}Fe_{1-y}O_{3-\delta}$ are less than that of $La_{1-x}Mn_{1-y}O_{3-\delta}$. A Pt-O layer exists on the Pt surface. The existence of O adatoms on the Pt surface may impact the methanol adsorption process. The O adatoms will reduce the tendency of the Pt surface as an electron donor for the H-Pt bond. Therefore, the energy barrier for breaking of the O-H bond may be increased. The present *ab initio* atomistic simulation did not take into account the impact of Nafion ionomer to the electrocatalysis process. In fact, although there is evidence that the ionomer affects the elementary electrochemical processes including adsorption and bond breaking, no systematic study has been done so far and discussions on the implication of the ionomer in confined to its enhancement of the ionic conductivity.

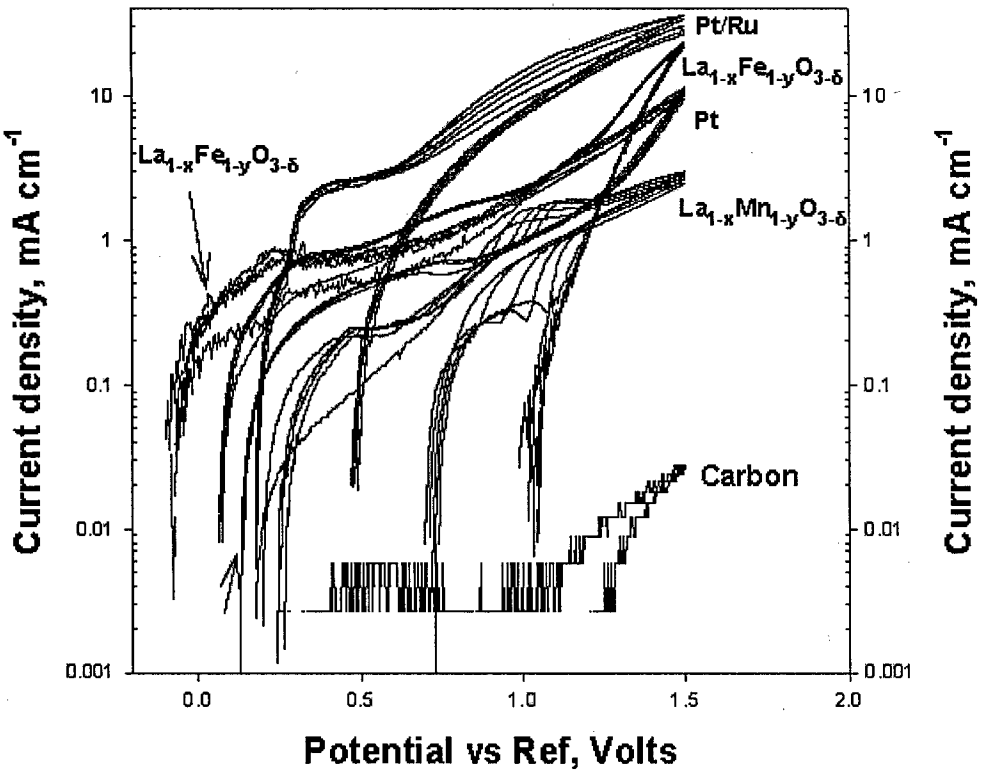

Figure 20. Cyclic voltametry curves for carbon, $La_{1-x}Mn_{1-y}O_{3-\delta}$, Pt, $La_{1-x}Fe_{1-y}O_{3-\delta}$, and Pt/Ru catalysts in 1 M methanol solution.

Table 4. Values of methanol oxidation onset potential and apparent exchange current density for Pt-Ru/C, $La_{1-x}Fe_{1-y}O_{3-\delta}$, Pt/C, $La_{1-x}Mn_{1-y}O_{3-\delta}$, and carbon.

Electrocatalyst material	Methanol oxidation onset potential / V vs. Ref.)	Apparent exchange current density / A cm^{-2}
Pt-Ru/C	0.4	$1.0x10^{-3}$
$La_{1-x}Fe_{1-y}O_{3-\delta}$	0.2	$5.0x10^{-4}$
Pt/C	0.3	$3.0x10^{-4}$
$La_{1-x}Mn_{1-y}O_{3-\delta}$	0.45	$1.0x10^{-4}$
Carbon cloth	>1.2	$<10^{-6}$

Scanning tunneling microscopy (STM) study

Figure 21 shows the topographic images of the deposited platinum in a different resolution. The lower resolution STM images of Pt deposits grown within the potential window used in this work are characterized by a number of separate Pt agglomerates and large, bare HOPG surface domains. At the nanometer level, the sample contains many Pt nanoparticles about 5 nm in size with some conglomeration. The individual Pt particle is ellipsoidal with no apparent facets. In our observations, no flat, triangular Pt crystals were observed, which was different from previous results in the literature [18]. Figure 21c shows that the surface of the nano-crystals has some roughness or some plateaus and steps. This surface steps form many dangling bonds that may facilitate the adsorption and bond breaking of fuel molecules and in this way enhance the activity of the electrocatalysts. An atomic level image was taken of the large individual Pt particle. Figure 21d shows the atomic image of deposited Pt (2.5nm×2.5nm). It shows a distorted hexagonal pattern and the average interatomic distance is 2.7±0.2Å, which is in agreement with the atomic distance (2.77 Å) of Pt. We also examined the Pt particles deposited from 10 mM H_2PtCl_6 with 0.5 M H_2SO_4 as a supporting solute. Figure 22 is the STM image of Pt deposited at –180 mV bias voltage for 30 s. The Pt particles are larger than those deposited without a supporting solute, and through growth, many particles have combined into larger ones without clear grain boundaries. It is expected that large Pt particles with flat shapes can be attained in a longer time deposition with H_2SO_4 serving as supporting solute. This study demonstrates that high surface area Pt catalysts can be produced using the electrochemical deposition method. In order to achieve a high effectiveness of the electrocatalysts, in addition to high surface area, good compatibility of the ionic conductor or ionomer and the electrocatalysts is very important.

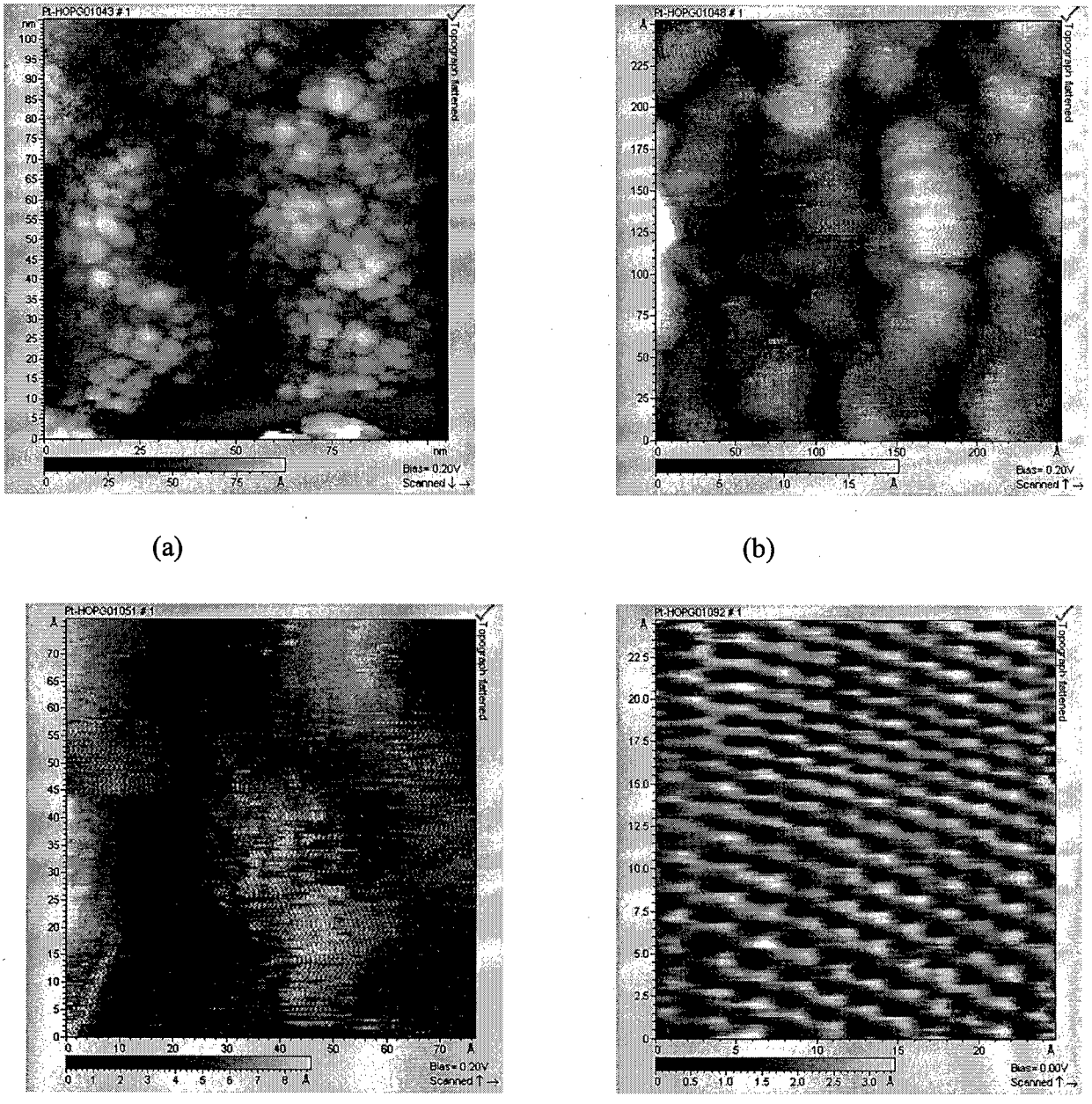

Figure 21. Topographic images of platinum particles deposited in 10 mM H_2PtCl_6 without supporting solute.

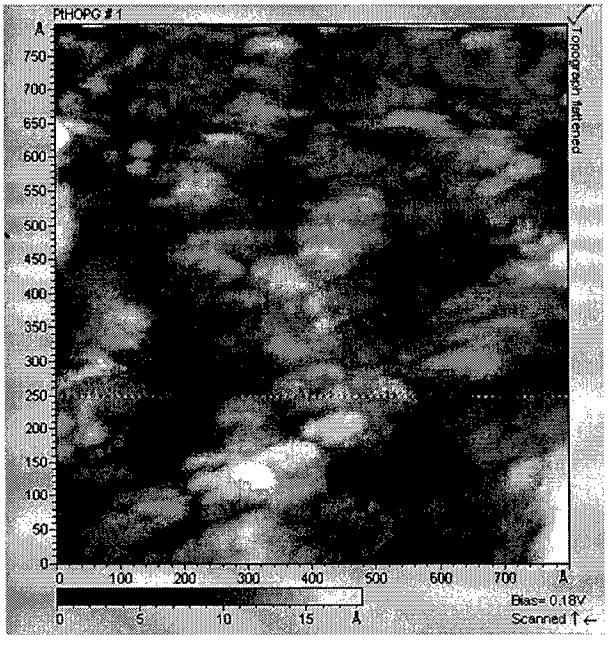

Figure 22. Topographic image of platinum particles deposited in 10 mM H_2PtCl_6 with 0.5 M H_2SO_4 as a supporting solute.

Current sensing atomic force microscopy (CSAFM) measurements

The sample for this measurement is in fact a tiny membrane electrode assembly (MEA) with a counter electrode. Thus, a porous Pt-coated support is coated with a polymer electrolyte membrane. Pt particles mixed with Nafion ionomer are deposited on the polymer electrolyte film. The CSAFM with a conductive tip (Pt, Au or Ag coated) allows determination of the size and morphology of the electrocatalysts and determination of the polarization and interface impedance. As shown in Figure 23, the image on the left is the topography of the Pt particles with the ionomer on the Nafion membrane. The image at the middle is the AFM current signal distribution in the same area. The letters from A to E denote the specific spots where the AFM tip was put for electrochemical measurements. The graphs A, B, C, D, and E at the bottom are dynamic polarization curves that were evaluated the spots A, B, C, D, and E respectively. Spots C and D were at the perimeters of the Pt particle and dark areas that are supposed to be the ionomer domains. Spots A, B, and C are at the top of the Pt particles. Only the polarization curves generated at spot C and D show some electrochemical activity. These results indicate that only the catalyst surface area that is close to or covered with ionomer is effective. If the area is 50-100 nm away from the ionomer, the distance prevent charge transfer from the reaction sites on the electrocatalysts to the electrolyte, resulting in termination of the reaction.

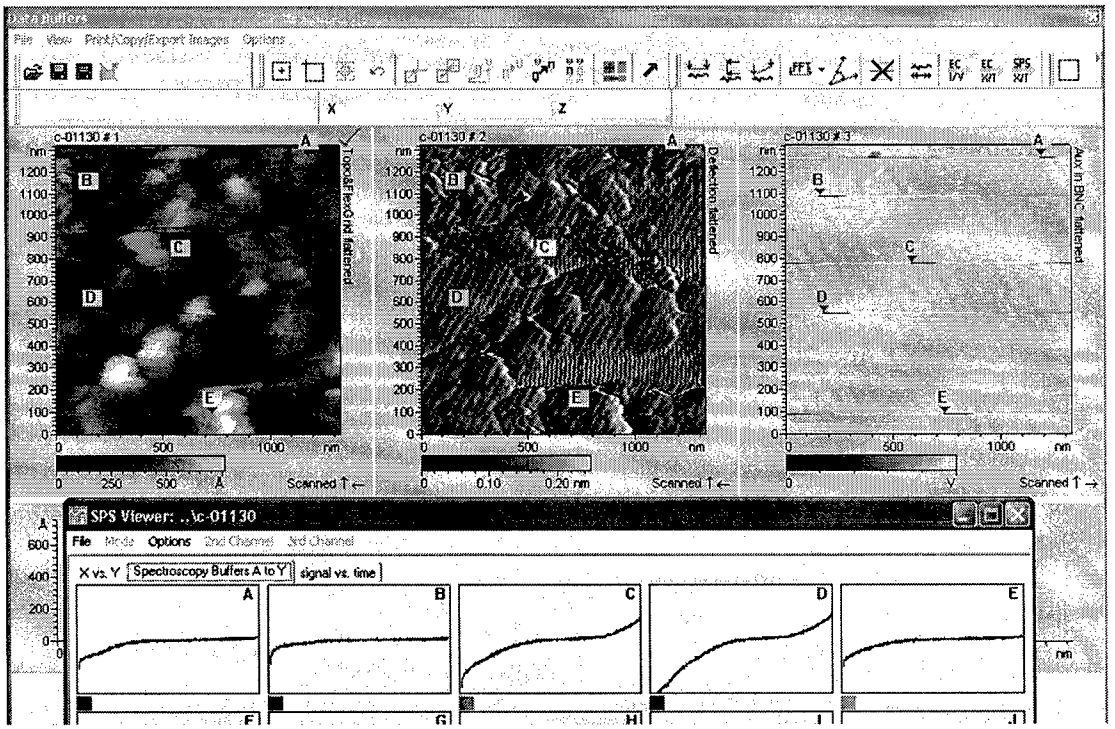

Figure 23. CSAFM imaging on a Nafion membrane with Pt/C/Nafion electrocatalyst particles. On top, are the CSAFM images. On the bottom, are the polarization curves for different positions on the Nafion membrane. Only the two positions on the Pt/C/Nafion particles show electrochemical activity.

4.4 Conclusions

According to the project plan, we have accomplished:

8) molecular dynamic simulation of the transport processes in Nafion 117 membranes;
9) development of experimental systems for conductivity and permeability measurement in a wide range of temperature and relative humidity;
10) synthesis of a new type of proton exchange membrane, ABPBI,
11) *ab initio* atomistic simulation of the electrocatalysis processes;
12) development of a high throughput method for evaluating the activity of electrocatalysts;
13) Examination of the Pt electrocatalysts using scanning tunneling microscopy;
14) Exploration of use current sensing atomic force microscopy for evaluating the intrinsic electrochemical activity of electrocatalysts.

As the first attempts, the present molecular dynamic simulations are in good agreement with the experimental results at room temperature. The simulations very precisely predict the

permeabilities of hydroniums and methanol in a temperature range between 20 and 120°C. However the computational conductivity results gradually deviate from the experimental values with increasing temperature. Overall, the deviations were much less than one order of magnitude in wide ranges of temperature and humidity. Thus, with further revision and optimization, the molecular dynamic simulation can be used for predicting the transport properties of the proton exchange membranes and help design novel high performance proton exchange membranes. The new APPBI membranes are stable at temperature to 110°C. The permeability of methanol in the ABPBI membranes is much lower than that in the Nafion 117 membrane. The PBI membrane is thus promising for use as the polymer electrolyte in a high temperature proton exchange membrane fuel cell.

The methods that we used for the *ab initio* atomistic simulations included establishment of the initial and final surface configurations for the electrochemical reactions, configuration optimization, and linear synchronous transit (LST) and quadratic synchronous transit (QST) computations. This method allows direct evaluation of the energy barriers for electrochemical reactions. The computational results correlate with the experimental results. However, this computation requires a high performance computer and long computational time. It is desired that these methods are implemented in a supercomputer, allowing examination of many other materials as electrocatalysts.

The CSAFM study is the first attempt to evaluate the intrinsic electrochemical activity of electrocatalysts. The results clearly demonstrate that on the catalyst surface areas that are about 20 nanometers to the ionomer are active and the surfaces 50-100 nanometer from the ionomer are not active at all. Only the active sites in these areas actually contribute to the electrocatalysis in a fuel cell electrocatalyst layers.

4.5 References

1. Michael P. Allen, Introduction to Molecular Dynamics Simulation published in Computational Soft Matter: From Synthetic Polymers to Proteins, Lecture Notes, Norbert Attig, Kurt Binder, Helmut Grubm¨ uller, Kurt Kremer (Eds.), John von Neumann Institute for Computing, J ¨ ulich, NIC Series, Vol. 23, ISBN 3-00-012641-4, pp. 1-28, 2004.
2. A.B. Anderson, "Theory at the electrochemical interface: reversible potential and potential-dependent activation energies". Electrochimica Acta 48, 3743-3749 (2003).
3. M.L. Machesky, "Influence of temperature on ion adsorption by hydrous metal oxides, in Chemical Modelling of Aqueous Systems II, D.C. Melchior, R.L. Basset (Eds.)", American Chemical Symposium Series 416, 282-292(1990).
4. Ken Onda, Bin Li, Jin Zhao, Kenneth D. Jordan, Jinlong Yang, Hrvoje Petek, "Wet Electrons at the H2O/TiO2(110) Surface", Science, 308, 1154-1158 (2005).
5. N.J. Tao, C.Z. Li, and H.X. He, J. Electroanal Chem 492, 81-93 (2000).
6. Adam Z. Weber and John Newman, "Transport in Polymer-Electrolyte Membranes, I. Physical Model", Journal of The Electrochemical Society, 150 (7), A1008-A1015 (2003).
7. Adam Z. Weber and John Newman, "Transport in Polymer-Electrolyte Membranes, II. Mathematical Model", Journal of The Electrochemical Society, 151(2), A311-A325 (2004).
8. Xiangyang Zhou, Jamie Weston, Elena Chalkova, Michael A. Hofmann, Catherine M.

Ambler, Harry R. Allcock, and Serguei N. Lvov, "High Temperature Transport Properties of Polyphosphazene Membranes for Direct Methanol Fuel Cells", Electrochimica Acta 48, 2173-2180 (2003).
9. M. V. Fedkin, X.Y. Zhou, M. A. Hofmann, Elena Chalkova, Jamie Weston, H. R. Allcock, and S. N. Lvov, "Experimental measurements of the diffusion coefficients of methanol in proton-conducting polyphosphazene membranes", Materials Letters, 52, 192-196 (2002).
10. Accelrys, http://www.accelrys.com/about/msi.html
11. K.L.Yeung, E.E. Wolf, J.Catal. 13, 135(1992).
12. S. Lee, H. Permana, K.Y. Ng Simon, J.Vac.Sci.Technol. B10, 561 (1992).
13. S. Gao, L.D.J. Schmidt, J.Catal. 115, 356 (1989).
14. W.A. Egli, A. Visintin, W.E. Triaca, A.J. Arvia, Appl.Surf.Sci. 68, 583 (1993).
15. M.L. Satter, P.N. Ross, Ultramicroscopy, 20, 21 (1986).
16. M. Watanabe, H. Sei, P. Stonehart, J.Electrochem.Soc. 261, 375 (1989).
17. O.M. Mognussem, J. Hotlos, R.J. Nichols, D.M. Kolb, P.J. Belm, Phys.Rev.Lett. 64, 2929 (1990).
18. J.L. Zubimendi, L.Vazquez, P. Ocon, J.M. Vara, W.E. Triaca, R.C. Salvavezza, A.J. Arvia, J.Phys.Chem. 97, 5095 (1993).
19. M.P. Green, K.J. Hanson, R. Carv, I. Lindau, J.Electrochem.Soc. 137, 3493 (1990).
20. I. Oda, Y. Shingaya, H.Matsumoto, M. Ito, J.Electroanal.Chem. 409, 95 (1996).
21. J.V. Zoval, R.M. Stiger, P.R. Biernack, R.M. Penner, J.Phys.Chem. 100, 837 (1996).
22. I. Lee, K.Y. Chan, D.L. Phillips, Appl.Surf.Sci. 136, 321 (1998).
23. E.H. Sanders a, K.A. McGradya,1, G.E. Wneka, C.A. Edmondsonb, J.M. Mueller b, J.J. Fontanella b,2, S. Suarez c, S.G. Greenbaum, "Characterization of electrosprayed Nafion films", Journal of Power Sources, 129, 55-61 (2004).

5.0 Personnel Supported

Dr. Xiangyang (Joe) Zhou, Project Manager
Dr. Zhen Chen, Research Scientist
Dr. George Philippidis, Sr. Program Manager
Ms. Bail Hu, Lab Manager
Satyen Thaker, Master student
Yong Gao, PhD. student
Francisco Delgado, undergraduate student
Dan Brenner, undergraduate student.

6.0 Publications

One manuscript has been drafted and is under internal review for submission to *Electrochimica Acta.*

1. X. Zhou, Z. Chen, F. Delgado, D. Brenner, and R. Srivastava, "Atomistic dynamic simulation of transport properties in polymer electrolyte fuel cells and experimental validation", the 208th Meeting of the Electrochemical Society, Los Angeles, Ca, Oct. 2005.

2. X. Zhou and F. Zhang, "Deposition and imaging of Pt Nanocrystals on highly oriented pyrolytic graphite", the 208th Meeting of the Electrochemical Society, Los Angeles, Ca, Oct. 2005.
3. Xiangyang Zhou , Baili Hu, Zhen Chen, Francisco Delgado, and Rajiv Srivastava, "Non-Precious Metal Perovskite Electrocatalysts for Direct Methanol Fuel Cells", Electrochemical and Solid-State Letters, Accepted for publication.
4. X. Zhou, Z. Chen, F. Delgado, D. Brenner, and R. Srivastava, "Molecular dynamic simulation of methanol diffusion in Nafion polymer electrolyte", submitted to ECS Transactions.

7.0 Interactions/Transitions

Participation/presentations at meetings, conferences, seminars

AFOSR and ONR Joint Program Review Meeting, May 2004.
AFOSR Program Review Meeting, March 2005.
The 208th Electrochemical Society Meeting, 2005

Consultative and advisory functions to other laboratories and agencies

None in this period.

Transitions

None in this period.

8.0 New discoveries, inventions, or patent disclosures.

1) A new high temperature proton exchange electrolyte or membrane, APPBI.
2) New non-precious metal oxide electrocatalysts for direct methanol fuel cells.

9.0 Honors/Awards

None during this reporting period.